Exp Fluids (2007) 42:941–954
DOI 10.1007/s00348-007-0305-3

RESEARCH ARTICLE

Experimental investigation of planar offset attaching jets with small offset distances

Nan Gao · Dan Ewing

Received: 27 August 2006 / Revised: 28 March 2007 / Accepted: 30 March 2007 / Published online: 26 April 2007

Abstract An experimental investigation was performed to characterize the development of planar jets initially issuing parallel to an adjacent wall with offset distances of up to 1 jet height and Reynolds number of 44,000. The results showed that the initial development of the mean flow field in the planar offset jets could be divided into five regions; three associated with the jet attaching to the wall similar to other reattaching shear layer flows and two associated with the resulting planar wall jet flow. The transition from the reattaching flow to the wall jet flow was also characterized by a significant change in the characteristic frequency, size, and convection velocity of the large-scale structures in the flows.

List of symbols

C_P	mean wall pressure coefficient, $2(P–P_\infty)/\rho\ U_a^2$
$C_{p'}$	fluctuating wall pressure coefficient, $2p'/\rho\ U_a^2$
f	frequency, Hz
F_{pp}	power spectrum of the fluctuating pressure, Pa^2/Hz
H_s	offset distance from the lower edge of the jet outlet to the wall, m
H_j	height of the jet, m
P	mean pressure, Pa
p'	RMS value of the fluctuating wall pressure, Pa
Re	Reynolds number of the jet, U_aH_j/v
U	streamwise component of the local mean velocity, m/s
$U_{\max}$	maximum local mean streamwise velocity, m/s
U_a	flow rate averaged velocity of the jet at the exit, m/s
u'	RMS value of the streamwise fluctuating velocity, m/s
$u'_{\max}$	maximum u' along the inner shear layer, m/s
$\langle uv \rangle$	turbulent Reynolds shear stress, m^2/s^2
W	channel or facility width, m
X_r	attachment length, m
x	spatial coordinate in the streamwise direction, m
x_1	location of the reference microphone in the two-point measurements, m
x_2	location of the second microphone in the two-point measurements, m
y	spatial coordinate in the vertical direction, m
$y_{+1/2}$	outer half width of the jet, m
z	spatial coordinate in the cross-stream direction, m
θ_o	initial momentum thickness of the jet shear layer, m
v	kinematic viscosity of air, m^2/s
ρ	density of air, kg/m^3
ρ_{pp}	correlation coefficient of the fluctuating wall pressure
ρ_{pu}	correlation coefficient of the fluctuating wall pressure and the streamwise fluctuating velocity
ρ_{pv}	correlation coefficient of the fluctuating wall pressure and the vertical fluctuating velocity
τ	time interval, s

The research was funded by the Natural Sciences and Engineering Research Council of Canada.

N. Gao · D. Ewing
Department of Mechanical Engineering,
McMaster University, Hamilton, ON, Canada L8S 4L7

Present Address:
N. Gao
School of Engineering, Sun Yat-sen University,
Guangzhou 510275, China

D. Ewing (✉)
Queens University, Department of Mechanical
and Materials Engineering, Kingston, Canada
e-mail: ewing@queensu.ca

1 Introduction

Turbulent planar jets that are initially travelling parallel to an adjacent wall can effectively form a barrier between an outer flow and the wall or cause a maximum in the local convective heat transfer rate when they attach to the wall, making them useful in a range of thermal management applications. Previous investigations have characterized the Reynolds averaged flow fields in turbulent offset planar jets analytically (Bourque and Newman 1960; Sawyer 1963; Bourque 1967), experimentally (Sawyer 1960; Hoch and Jiji 1981; Lund 1986; Pelfrey and Liburdy 1986; Nasr and Lai 1997, 1998), and numerically using RANS models (Nasr and Lai 1998). The heat transfer from the wall to the flow has also been considered (Kim et al. 1996; Song et al. 2000). Most of these investigations focused on jets with initial offset distances larger than the jet height (H_j). In these cases, the ratio of the reattachment length (X_r) of the offset jets to the offset distance (H_s) decreases as the offset distance increases in agreement with the model proposed by Bourque (1967) for fully developed turbulent attaching jets.

There have been fewer investigations of jets with small offset distances where the jet interacts with and attaches to the wall in the near field of the jet, typical of the cooling jets used in the blown film manufacturing process (cf Gao et al. 2005; Gao and Ewing 2005) that motivated this investigation. In that application, there is also often a second co-flowing jet between the main jet and the wall that affects the interaction of the main jet with the wall. This investigation focusses on the development of a single offset jet to better understand the effect that the offset distance has on the development of the offset jet. The effect of adding a co-flowing jet will be considered elsewhere.

Heretofore, there does not appear to have been any investigations that have characterized the flow field in offset jets with small offset distances (less than H_j). Lund (1986) did characterize the reattachment length for offset jets with a wide range of offset distances, including small distances. There was good agreement with Bourque's model for the jets with large offset distances, but not for small offset distances. The ratio of the reattachment length to the offset height continued to change with the offset distance even for distances as small as 0.4 H_j.

There also does not appear to have been any investigations that have examined the dynamics of the large-scale structures in offset jets for any offset distance. The large-scale motions in the offset attaching jets with small offset distances should initially have features in common with other reattaching shear layer flows, such as flows over backward facing steps (e.g. Farabee and Casarella 1986; Driver et al. 1987; Heenan and Morrison 1998; Lee and Sung 2002; Spazzini et al. 2001) or flows separated from bluff fore bodies (e.g. Kiya and Sasaki 1983, 1985; Cherry et al. 1984; Hudy et al. 2003). The structures in these flows are often characterized using measurements of the fluctuating pressure or the fluctuating shear stress on the wall below the reattaching shear layer. The spectra near the reattachment location have a characteristic frequency at $fX_r/U_\infty \approx 0.5$–1 (e.g. Kiya and Sasaki 1983; Cherry et al. 1984; Farabee and Casarella 1986; Heenan and Morrison 1998; Lee and Sung 2002; Hudy et al. 2003; Spazzini et al. 2001) that is associated with the passage of the large-scale structures in the shear layer. The fluctuations near the separation point also often have a lower characteristic frequency of $fX_r/U_\infty \approx 0.1$ (e.g. Kiya and Sasaki 1985; Cherry et al. 1984; Castro and Haque 1987; Driver et al. 1987; Heenan and Morrison 1998) that is associated with the 'flapping' of the shear layer or a fluctuation in the size of the recirculating flow region. These low frequency fluctuations are not observed in all cases (e.g. Chandrsuda and Bradshaw 1981; Ruderich and Fernholz 1986), but modulate the structures in the shear layer when they are present (e.g. Kiya and Sasaki 1985; Cherry et al. 1984; Heenan and Morrison 1998).

The interaction between the different motions will be further complicated in offset attaching jets by the presence of the large-scale structures in the outer shear layer of the jet. The structures from the reattaching shear layer will also affect the large-scale structures in the wall jet downstream of the reattachment point. The wall pressure fluctuations are related to the turbulent fluctuations in the flow field through a Poisson equation and thus can be used to characterize the transition between the different motions as the flow develops. The pressure fluctuations are also of practical interest for the blown-film manufacturing application, where the jets cool a pliable thin plastic film, because flow-induced vibrations occur even for moderate speed jets considered here. Thus, space and time resolved measurements of the fluctuating wall pressure below the offset jets will provide insight into the nature of the dynamic loading that occurs on the film in this application.

This investigation examines the flow field and the large scale structures in planar offset turbulent attaching jets exiting long channels with small offset heights, up to H_j, and Reynolds number of 44,000. The experimental facilities and methodology used in this investigation are outlined in the next section. Single-point measurements of the flow field are then presented. This is followed by measurements of the fluctuating wall pressure and the correlation between the fluctuating wall pressure and the fluctuating velocity that are used to characterize the large-scale structures present in the flow.

2 Experimental methodology

The development of the planar offset jets in this investigation was examined using the two jets exiting the long channels in the facility shown in Fig. 1. The air flow supplied from a variable speed blower was split into five hoses that led to a large upper settling chamber ($122 \times 72.4 \times 45.7$ cm), and three hoses that led to a smaller lower settling chamber ($81.3 \times 40.6 \times 22.9$ cm). The hose connections included gate valves to block flow to the channel not in use. The exit of the channel not in use was also sealed using tape to create a uniform boundary condition. Both settling chambers included layers of foam and perforated plates to condition the flow before it entered the channel. The facility initially included bell mouths at the channel entrances, but the exit profiles were uniform across more of the channel for square channel entrances that promote turbulence at the entrance. The height of the channel outlet (H_j) was 3.8 cm for the upper channel and 1.8 cm for the lower channel. The width of the channels and the facility into the page (W) was 74.3 cm, so the ratio of the channel width to height (W/H_j) was 19.5 for the upper channel and 41 for the lower channel. The length of the upper channel was 81 cm or 21.3 times the channel height, while the length of the lower channel was 50.8 cm or 28.2 times that channel height.

The jet exiting the channel in use developed over a 1.8 m long plate that was mounted parallel to the channels. The height of this plate could be adjusted to change the offset distance from the wall to the bottom of the channel outlet (H_s). The flow was also confined using an 80 cm high back wall and two 100 cm high by 180 cm long side walls. Most measurements reported here were performed using the upper channel (with $W/H_j = 19.5$) when the average velocity at the exit was 18.4 m/s. This corresponded to a Reynolds number based on jet height of approximately 44,000. Measurements were performed for Reynolds numbers of 20,000–50,000 for an offset distance of $0.4\,H_j$. Measurements of skin friction were also performed for the jet with $W/H_j = 41$ at a Reynolds number of 44,000, while the static and fluctuating pressure were also measured for the jet exiting this channel when $H_s/H_j = 1$. The results from the two jets agreed as discussed below.

The profiles of mean velocity and turbulent stresses measured at the exit of the two channels were symmetric and fully developed. In particular, the Reynolds shear stress $\langle uv \rangle$ varied linearly across the core region of the flow at the exit. The profiles measured along the upper channel outlet were uniform over the central region of the jet from $-6 \leq z/H_j \leq 6$, where z is the coordinate out of the page in Fig. 1. The variations in the mean and rms velocities were within ±1 and ±2.5%, respectively, that were within experimental uncertainty. The effect that the side walls had on the development of the jet was examined by measuring profiles across the jet as discussed below.

The reattachment location of the jets, defined in terms of the location of zero mean shear stress, was determined using a surface oil flow visualization technique (cf Naughton and Sheplak 2002). In this approach, Dow Corning 200 fluid was applied to the surface. The jet was then run at the desired condition, while the oil was illuminated using a single wavelength light source and observed using a CCD camera. Once the reattachment location was evident in the resulting fringe pattern, the jet was stopped and the reattachment length was measured using a ruler with a resolution of 1 mm. The repeatability of the reattachment locations determined through multiple runs was less than 8% for jets with $H_s/H_j = 0.1$ and 3% for jets with $H_s/H_j = 1.0$. The major source of this variability was attributed to measurement uncertainty.

The development of the flow field in the offset jets was characterized using single and cross hot-wire probes with an in-house anemometry system based on the designs proposed in Perry (1982) and Citriniti (1996). The sensor in the single-wire probe had a diameter of 5 μm and a length of 1.25 mm, while the sensors in the cross-wire probe were 1.5 mm long. The hot wire probes were calibrated in a separate facility using a jet exiting a contoured nozzle that

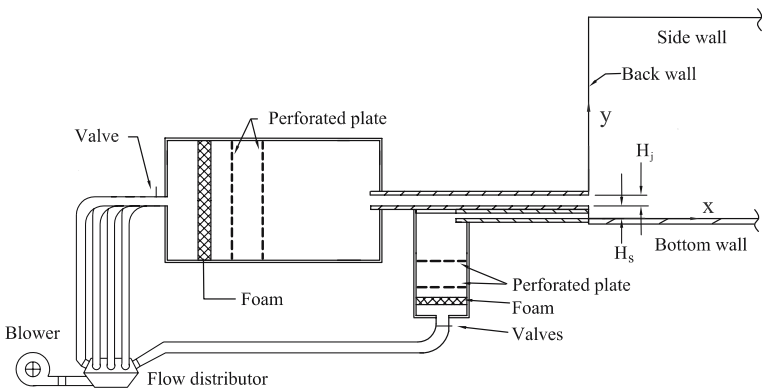

Fig. 1 Schematic of the experimental facility

had a uniform exit velocity profile. The resulting response curves were fit with a four-order polynomial, and a modified cosine law (Bruun 1995).

The flow field was measured by moving the hot-wire probe on a computer controlled traverse that could be positioned with an accuracy better than 0.05 mm. At each point, the output signals from the anemometers were sampled using a 14-bit A/D board at a frequency of 4,096 Hz for a total time of 50 s. The uncertainties in the mean velocity and rms velocity measurements due to sample size, evaluated following the approach in Bruun (1995), were less than 1 and 3%, respectively, for a 95% confidence interval. The ambient air temperature during the measurements was measured using an RTD temperature sensor with a resolution of 0.1°C. The temperature varied less than ±1 °C and the effect of the temperature change on the velocity measurements was compensated using the technique proposed by Beuther (1980).

Rectification in the hot-wire measurements was examined using the probability density function of the instantaneous fluctuating velocity for the single-wire measurements and using the phase diagram of the effective cooling velocities for the cross-wire measurements (Tutu and Chevary 1975). Rectification affected less than 1% of the data points for the single-point results reported here (other than the outer most points in the exit profiles) that were taken from the single-wire measurements. Rectification affected less than approximately 2.5% of the data in the cross-wire measurements used for the pressure velocity correlations at the inner half-width. The estimate of the cross-flow error in the single-wire measurements in the attaching shear layer were 3–4% for the mean velocity and 15–20% for the rms fluctuating streamwise velocity at the inner half-width near reattachment. The cross-flow error was smaller upstream of this point and at the outer half-width.

The mean pressure on the bottom wall was measured using a calibrated differential pressure transducer at a series of pressure taps mounted along the jet centerline. This included 8 equally spaced taps between x/H_j = 0.25 and 2 and 16 equally spaced taps between x/H_j = 2.5 and 12. The fluctuating static pressure on the bottom wall was measured using 16 Panasonic WM-60B microphones, that had flat responses for 20–5,000 Hz. The microphones were mounted directly into a series of blind cavities drilled from the bottom of the wall on a line that was 0.75 cm off the jet centerline. The microphones sensed the flow through a 1 mm-diameter, 5 mm-long pinhole drilled through the wall to the top of the cavity. There were 6 cavities at equally spaced locations between x/H_j = 0.25 and 1.5, 9 cavities at equally spaced locations between x/H_j = 2–6, and 3 cavities at equally spaced locations between x/H_j = 8 and 12. The locations used in the measurements were varied according to the offset height.

The microphones were calibrated externally using a piston phone at 1,000 Hz. The measurements for one case were compared with measurements performed using a different bottom wall where the microphones were flush mounted with the surface. The magnitude of the pressure fluctuations for the two configurations agreed to within 10%. The spectra also agreed up to 400 Hz that was above the frequencies of interest here. The lowest resonance frequency of the cavity observed in the measurements was 2,000 Hz. There was concern that the flush mounted microphones could affect the flow along the wall so that the measurements through the pinholes were used for all the results reported here. The ambient noise characterized by leaving one microphone out of the flow in a typical experiment was less than 1% of the rms fluctuating pressure measured in the wall jet region and a smaller fraction of the result in the reattaching region. The responses of these microphones were compared with a reference microphone using an acoustic chamber.

The signals from the microphones were simultaneously acquired with the 14-bit A/D board in 100 blocks of 4,096 data points at a frequency of 4,096 Hz. The uncertainties for the mean and fluctuating wall pressure due to the sample size were less than 2 and 4%, respectively, for a 95% confidence interval, while the uncertainties in the spectra were less than 20%, for a 95% confidence interval. The large-scale structures in the flow were further characterized by simultaneously measuring the velocity with the cross-wire probe and the fluctuating pressure on the wall using the microphones. The signals from the transducers were again acquired with the 14-bit A/D board in 100 blocks of 4,096 data points at a frequency of 4,096 Hz.

3 Results

Profiles of the mean velocity near the reattachment point in the offset jet with H_s/H_j = 0.6 are shown in Fig. 2. The mean velocities have been normalized using the average velocity at the jet exit, U_a, determined by integrating the velocity profiles measured at the exit. The results show that the bulk of the jet turns toward and then attaches to the wall. The location of the maximum mean velocity initially continued to approach the wall downstream of the reattachment location as the flow recovers to a wall jet. This was observed in all of the jets. The effect that the side walls in the facility had on the development of the jets was examined by measuring the development of the boundary layer on the side walls of the facility for the jet with H_s/H_j = 1. The thickness of these layers grew to approxi-

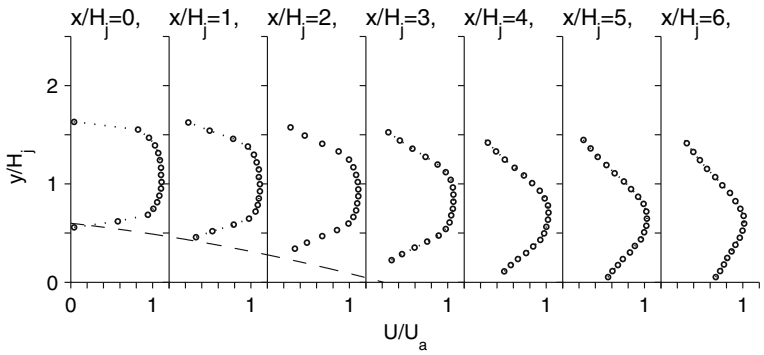

Fig. 2 Profiles of the mean streamwise velocity in the region $x/H_j \leq 6$ for the jet with $H_s/H_j = 0.6$

mately $5H_j$ at $x/H_j = 12$ and $7H_j$ at $x/H_j = 20$. Measurements of the velocity distribution on the plane $x/H_j = 12$ showed that the profiles of the mean and turbulent fluctuating velocity were uniform over the remainder of the jet.

The reattachment length for the jets with H_s/H_j between 0.1 and 1.2 are shown in Fig. 3. The reattachment locations determined for the two jets used here agreed to within experimental uncertainty. The normalized reattachment location X_r/H_s was approximately 6 for jets with $H_s \lesssim 0.3\,H_j$, similar to the results for a flow over a backward facing step (e.g. Eaton and Johnson 1981; Driver et al. 1987). The normalized reattachment length decreased gradually with offset ratio for jets with $H_s \gtrsim 0.3H_j$, similar to the results of Lund (1986). The reattachment lengths here were approximately 15% larger than those reported by Lund for a jet exiting a nozzle with a contoured lower surface without a wall above the nozzle outlet. Measurements of the reattachment length were also performed here for jets with H_s/H_j of 0.2–1 when the wall above channel outlet was not present. The reattachment length differed by less than 2% from the results when the wall was present,

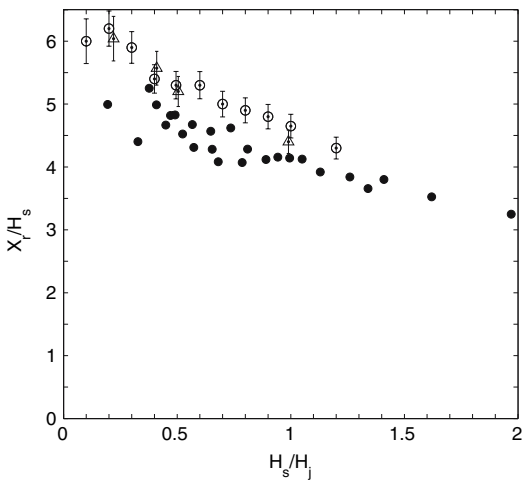

Fig. 3 Change in the reattachment location with offset height for *open circle* the jet with $W/H_j = 19.5$, *open triangle* the jet with $W/H_j = 41$, and *filled circle* reported by Lund (1986)

indicating that the differences between the results in this investigation and those reported by Lund were likely due to the difference in the nozzle shape rather than the presence of the wall behind the channel outlet. Similar size differences in the reattachment length were observed in jets exiting different nozzles with larger offset distances (e.g. Sawyer 1960; Nozaki et al. 1979, 1981; Nasr and Lai 1998).

The development of the jets with different offset distances can be compared by examining the change in the maximum mean velocity, $U_{\max}$, and in the outer jet half-width, $y_{+1/2}$, with downstream location shown in Figs. 4 and 5. Here, $y_{+1/2}$ is the distance from the wall to the outer location where the mean velocity is half the local maximum velocity. The results show that the development of the mean velocity field in the offset jets can be divided into five regions, three of which are associated with the reattaching flow region typical of other reattaching shear layer flows, and two of which are associated with the wall jet region. In the first region ($x/X_r \leq 0.65$), the maximum velocity is constant and the outer half width $y_{+1/2}$ decreases gradually as the jets curve toward the wall. The jets attach to the wall in the second region ($0.65 < x/X_r \leq 1.1$), which is characterized by a rapid decrease in both the jet half-width and the maximum velocity. The jet half width and the maximum velocity initially remain unchanged in the third region ($x/X_r > 1.1$) for the jets with small offset distances as the jets reorganize after attaching to the wall. The third region appears to end near $x/H_j \approx 6$ likely with the interaction between the outer and the inner shear layers or the end of the near field in the jet. The fourth region ($6 \lesssim x/H_j \lesssim 10$) is characterized by a rapid decrease in the maximum velocity and an increase in the jet half width, suggesting the flows transition to the wall jets. The jets appeared to undergo a transition to a fifth region near $x/H_j \approx 10$, characterized by an increase in the growth rate of the jet half-width in the planar wall jet and a decrease of the decay rate of the maximum velocity in the offset jet with $H_s/H_j = 1$. The height of the maximum velocity in these jets also reached a minimum near $x/H_j = 10$ providing further evidence that there was a change in the development of the wall jet flows.

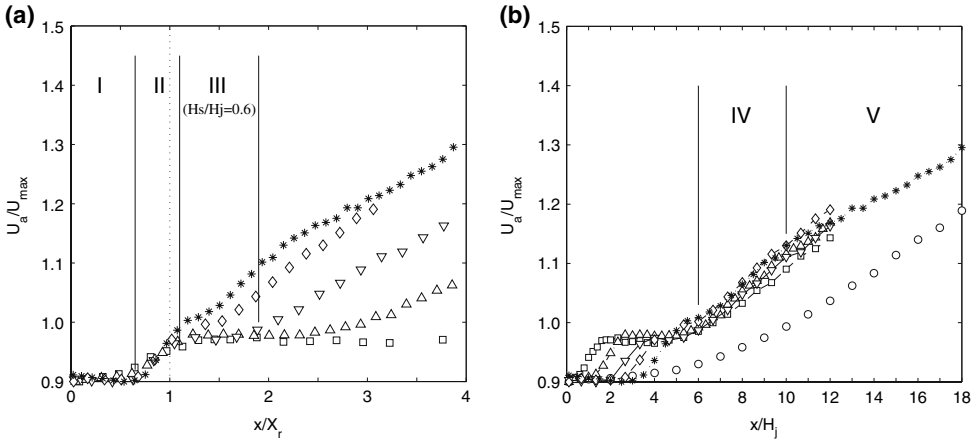

Fig. 4 Change in the maximum local mean velocity with streamwise distance for jets with H_s/H_j = *open circle* 0 *open square* 0.2 *open triangle* 0.4 *inverted open triangle* 0.6 *open diamond* 0.8 and *asterisk* 1

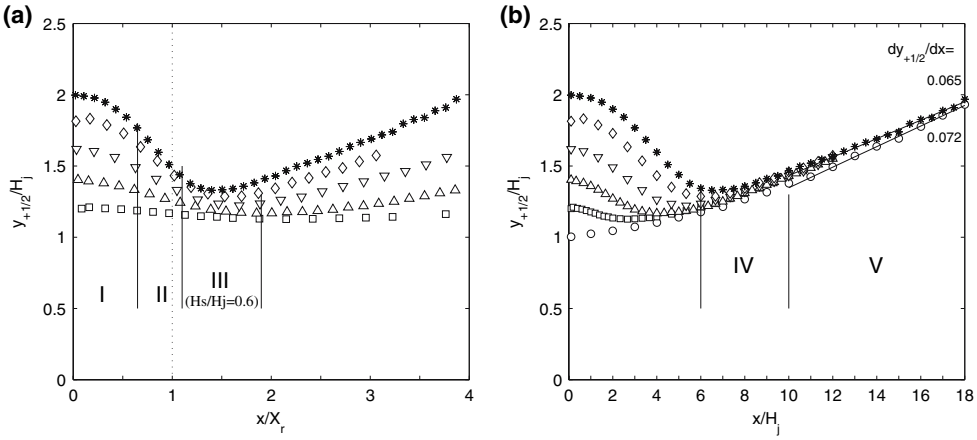

Fig. 5 Change in the outer jet half width with streamwise distance for jets with H_s/H_j = *open circle* 0 *open square* 0.2 *open triangle* 0.4 *inverted open triangle* 0.6 *open diamond* 0.8 and *asterisk* 1

The measurements were not extended downstream in all of the offset jets as the focus here was to examine the transition from the reattaching flow to the wall jet flow in the first four regions.

The change in the mean static wall pressure coefficient with streamwise position in the different offset jets is shown in Fig. 6. The results shown here for the jet with $H_j/H_s = 1$ exiting the channel with $W/H_j = 19.5$ agreed with results measured for the jet exiting the channel with $W/H_j = 41$. The static wall pressure decreases to a local minimum at $x/X_r \approx 0.65$ or the end of Region I as the jets initially curve toward the wall, before increasing rapidly through Region II to a maximum slightly downstream of the reattachment location as the flow turned away from the wall, similar to other attaching flows (e.g. Eaton and Johnson 1981; Farabee and Casarella 1986; Driver et al. 1987; Heenan and Morrison 1998). Both the maxima and minima in the static pressure coefficients increased when the initial offset distance of the jet increased due to the differences in the trajectory of the jet toward the wall. The mean wall pressure downstream of the reattachment point decreased to atmospheric pressure more gradually in the jets with the lower offset distances, indicating these jets recovered more gradually, consistent with the change in the maximum mean velocity observed in Region III, and there is a change in the development of mean flow downstream of the reattachment point with the offset height of the jet.

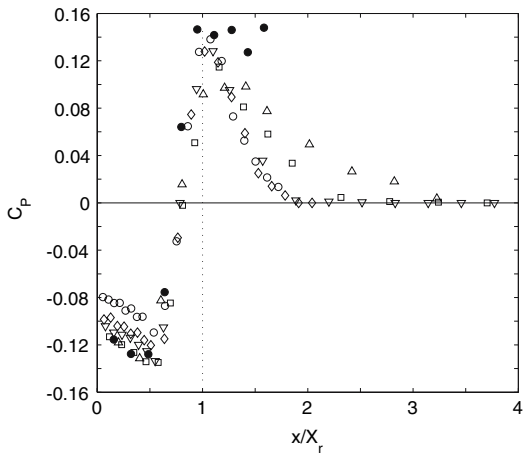

Fig. 6 Distributions of the static wall pressure coefficient for jets with H_s/H_j = *open triangle* 0.2 *open square* 0.4 *inverted open triangle* 0.6 *open diamond* 0.8 and *open circle* 1.0, and *filled circle* results from backward facing step (Heenan and Morrison 1998)

The fluctuating wall pressure coefficients shown in Fig. 7 collapse for $x/X_r \leq 0.65$ or Region I. Thereafter, the fluctuating pressure increased rapidly as the structures in the jets interacted with the surface, reaching a maximum slightly upstream of the reattachment location, similar to other reattaching flows. The maxima in $C_{p'}$ here are between the results for the backward facing step (e.g. Driver et al. 1987; Heenan and Morrison 1998) and those for the reattaching flow over a bluff body (e.g. Cherry et al. 1984; Hudy et al. 2003). The maximum in the fluctuating wall pressure coefficient increased from $C_{p'} \approx 0.03$ to 0.1 as the offset distance of the jet increased or the ratio of initial momentum thickness to the offset distance (θ_o/H_s) decreased, consistent with the measurements in the backward facing step (Eaton and Johnson 1981; Vogel and Eaton 1985; Heenan and Morrison 1998). The initial momentum thickness of the inner shear layer of the offset jets were all approximately 0.027 H_j, so the ratio of θ_o/H_s decreased from 0.14 to 0.027 as the offset height increased from 0.2 to 1. The ratio of θ_o/H_s did not change significantly for jets with Reynolds numbers between 22,000 and 55,000, and this change in Reynolds number did not have a significant impact on the magnitude of the wall pressure fluctuations. The fluctuating wall pressure downstream of the reattachment point in the offset jets eventually increases with downstream position similar to the planar wall jet flow suggesting that the turbulent fluctuations from the attaching shear layer give way to those associated with the wall jet flow. The local minima in the fluctuating pressure did not occur at a distinct downstream point indicating that the change in the structures did not necessarily correspond with the change in the evolution of the mean flow field observed in Figs. 4 and 5.

The profiles of rms streamwise fluctuating velocity measured in the offset jet with $H_s/H_j = 0.6$ are shown in Fig. 8. The magnitude of the turbulent fluctuations in the inner shear layer increases as the flow evolves downstream until the jet attaches to the wall. Thereafter, the turbulence fluctuations near the wall decrease due to the interaction with the wall. The change in the magnitude of the fluctuating velocity in the shear layers for the different jets can be compared by examining the change in the maximum value of the rms fluctuating velocity u'_{max} in the inner shear layers shown in Fig. 9. The results show that the size of the turbulence fluctuations in the inner shear layers of the offset jets increased rapidly reaching a maximum upstream of the reattachment location before decreasing downstream of the reattachment location. The size of the fluctuations in the inner shear layer near the reattachment location of the jet increased as the initial offset distance of the jet increased and the shear layer had longer to develop before it interacted with the wall.

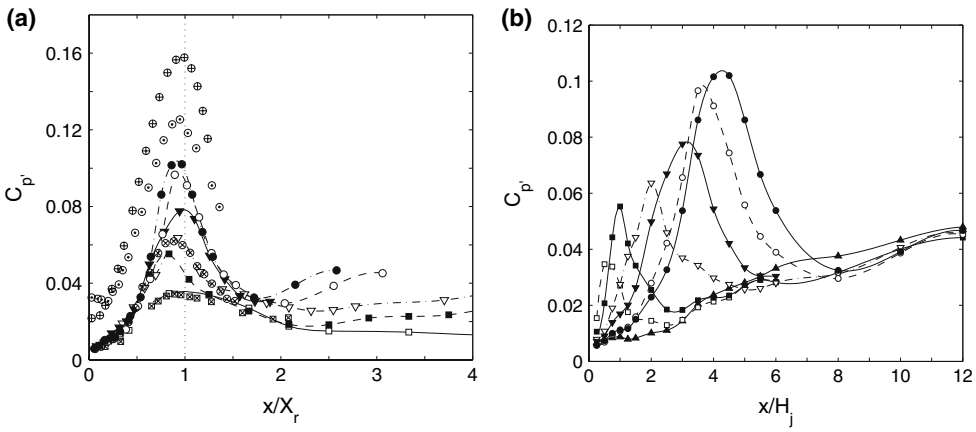

Fig. 7 Distributions of the fluctuating wall pressure coefficient for jets with H_s/H_j = *filled triangle* 0 *open square* 0.1 *filled square* 0.2 *inverted open triangle* 0.4 *inverted filled triangle* 0.6 *open circle* 0.8 *filled circle* 1.0, backward facing steps *squared times* Driver et al. (1987) *circled times* Heenan and Morrison (1998), and bluff body reattachment *circled dot* Cherry et al. (1984) *circled plus* Hudy et al. (2003)

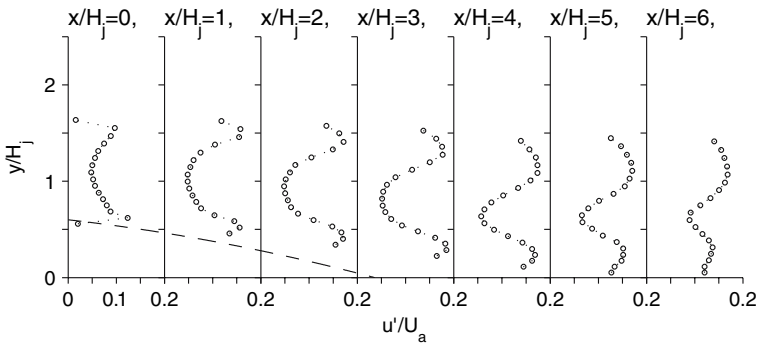

Fig. 8 Profiles of the rms fluctuating velocity in the region $x/H_j \leq 6$ for jet with H_s/H_j = 0.6

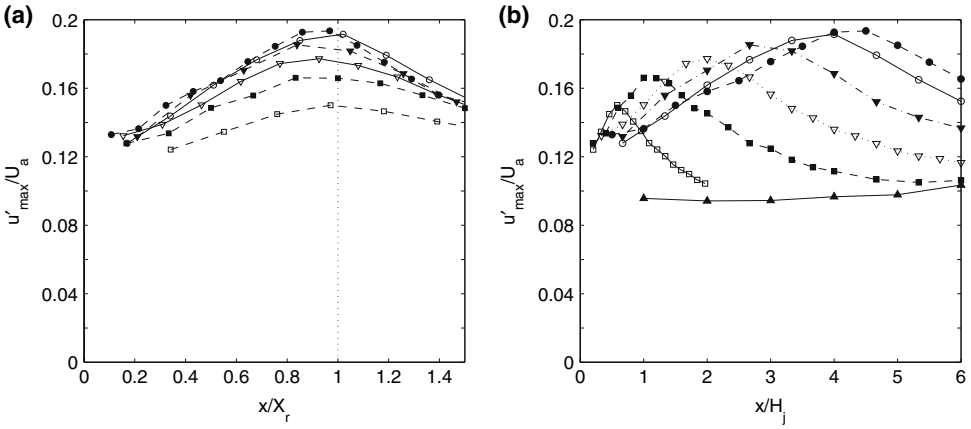

Fig. 9 Distributions of the maximum local rms fluctuating velocity in the inner shear layer for the jets with H_s/H_j = *filled triangle* 0 *open square* 0.1 *filled square* 0.2 *inverted open triangle* 0.4 *inverted filled triangle* 0.6 *open circle* 0.8 and *filled circle* 1.0

3.1 Measures of the large-scale structures

The wall pressure fluctuations are related to the turbulent fluctuations in the flow field through a Poisson equation and thus can be used to examine the change in the structures present in the flow as it evolves downstream. The spectra of the fluctuating wall pressure, F_{pp}, for jets with different offset distances are shown in Fig. 10. The pressure spectra at $x/X_r \lesssim 0.4$ show evidence of a significant low frequency peak at $fX_r/U_a \lesssim 0.2$, consistent with the previous measurements in some reattaching shear layer flows (e.g. Kiya and Sasaki 1985; Cherry et al. 1984; Driver et al. 1987; Heenan and Morrison 1998), that was also seen for the jet exiting the channel with $W/H_j = 41$. The precise frequency was difficult to determine here because it was near the lower end of the flat response region for the microphones. The spectra for frequencies below this range (< 20 Hz) are dotted here for clarity. Higher frequency peaks emerge at $x/X_r \approx 0.5$, similar to other reattaching shear layer flows. The frequencies of these peaks associated with the large scale flow structures in the attaching shear layer decrease as the flows evolve downstream. The characteristic frequency near the attachment point was fX_r/U_a = 0.5–1.0 (depending on the offset distance) consistent with the results near the reattachment location in other reattaching flows.

Fluctuations with the characteristic frequency associated with the reattaching shear layer persist in the pressure spectra until x/H_j = 6–8 but gradually disappear as the flow evolves downstream, unlike other reattaching

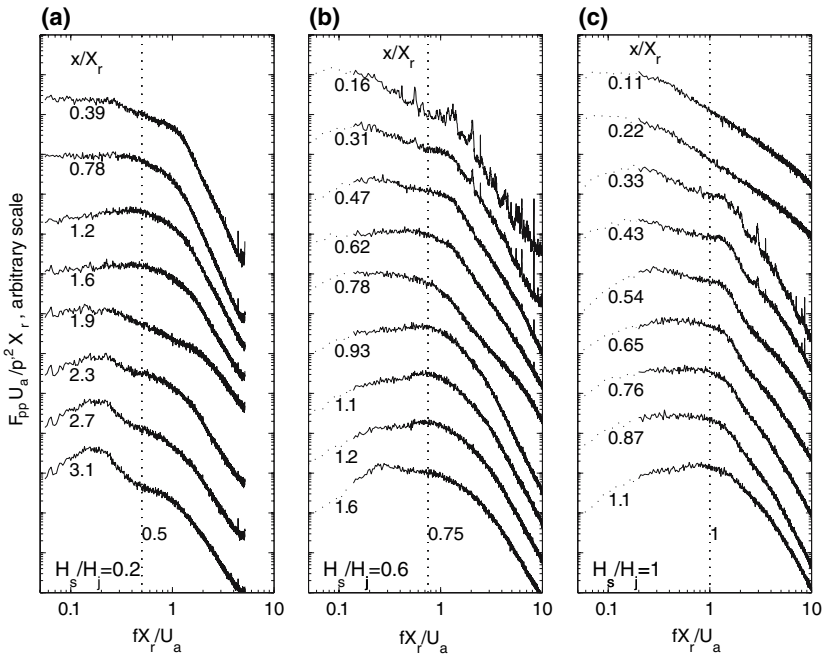

Fig. 10 Spectra of the fluctuating wall pressure normalized using length scale X_r for jets with H_s/H_j = **a** 0.2 **b** 0.6 and **c** 1.0

flows (e.g. Cherry et al. 1984; Hudy et al. 2003). A lower frequency peak also appeared upstream of this region. The spectra of the fluctuating pressure from the offset jets with H_s/H_j = 0.2 and 1 and the planar wall jet (H_s/H_j = 0) plotted in terms of fH_j/U_a are shown in Fig. 11. The pressure spectra from the offset jets have peaks at fH_j/U_a = 0.07–0.1 that began to emerge at x/H_j = 3–6 and dominate the spectra in the wall jet region. A similar peak occurs in the spectra from the planar wall jet for $x/H_j \geq 3$ suggesting the structures at this frequency are associated with the wall jet flow.

The correlation coefficients of the fluctuating pressure along the wall given by

$$\rho_{pp} = \overline{p(x_1,t)p(x_2,t+\tau)}/p'(x_1)p'(x_2), \quad (1)$$

for different points in the offset jet with H_s/H_j = 0.6 are shown in Fig. 12. The different regions of development in the mean flow defined previously are shown on this figure as a reference. The fluctuating wall pressures are well correlated in the different regions of mean flow development in this jet, but are not well correlated between the regions, indicating that the structures change as the flow evolves downstream. The propagation velocity of the pressure fluctuations also changed between regions. The propagation velocity of the most correlated fluctuations was determined from the slope of the locus of the main positive peak in the cross correlation contour given by (Heenan and Morrison 1998; Hudy et al. 2003)

$$\frac{U_c}{U_a} = \frac{\Delta x/H_j}{\Delta\tau U_a/H_j}, \quad (2)$$

where $\Delta x = x_2 - x_1$. The speed within each region was computed by selecting two locations, x_1 and x_2, within the region being considered. In region I, there was evidence of a downstream convection velocity of $U_c \approx 0.55U_a$, and an upstream convection velocity of $U_c' \approx -0.2U_a$ similar to the results of Heenan and Morrison (1998) and Hudy et al. (2003) in flows over a backward facing step and a bluff body, respectively. The propagation velocity in region II initially decreased to $U_c \approx 0.45U_a$ before increasing through the reattachment region reaching $U_c \approx 0.8U_a$ in Region III downstream of the reattachment point. The propagation velocity then decreased to $U_c \approx 0.6U_a$ at $x/H_j \gtrsim 6$ or Region IV, indicating again that there is a change in the passage of the large-scale motions as the flow travels from Region III to Region IV. The propagation velocity of $0.6U_a$ was similar to the velocity observed at $4 \leq x/H_j \leq 12$ in the planar wall jet (Fig. 13), where $U_c \approx 0.7U_a$.

The results indicate that the correlation coefficient of the fluctuating pressure along the wall can be used to characterize where the structures near the wall change from those associated with the attaching shear layer to those associated with the wall jet flow. Correlation coefficients of the fluctuating pressure measured downstream of the reattachment location in the jets with H_s/H_j = 0.2 and 1.0 are shown in Fig. 14. The correlation coefficient and the propagation velocity of the pressure fluctuations changed at

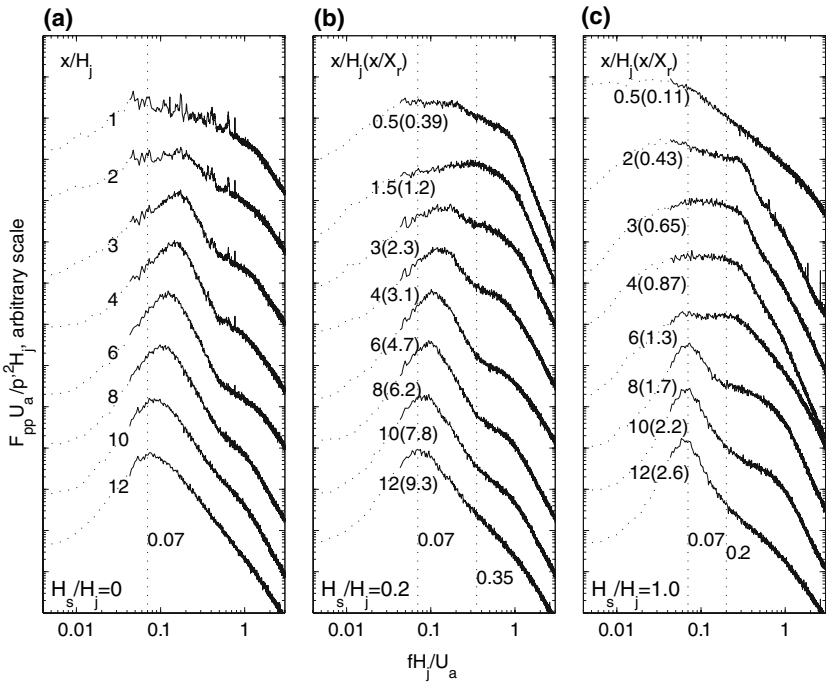

Fig. 11 Spectra of the fluctuating wall pressure normalized using length scale H_s for jets with H_s/H_j = **a** 0 **b** 0.2 and **c** 1.0

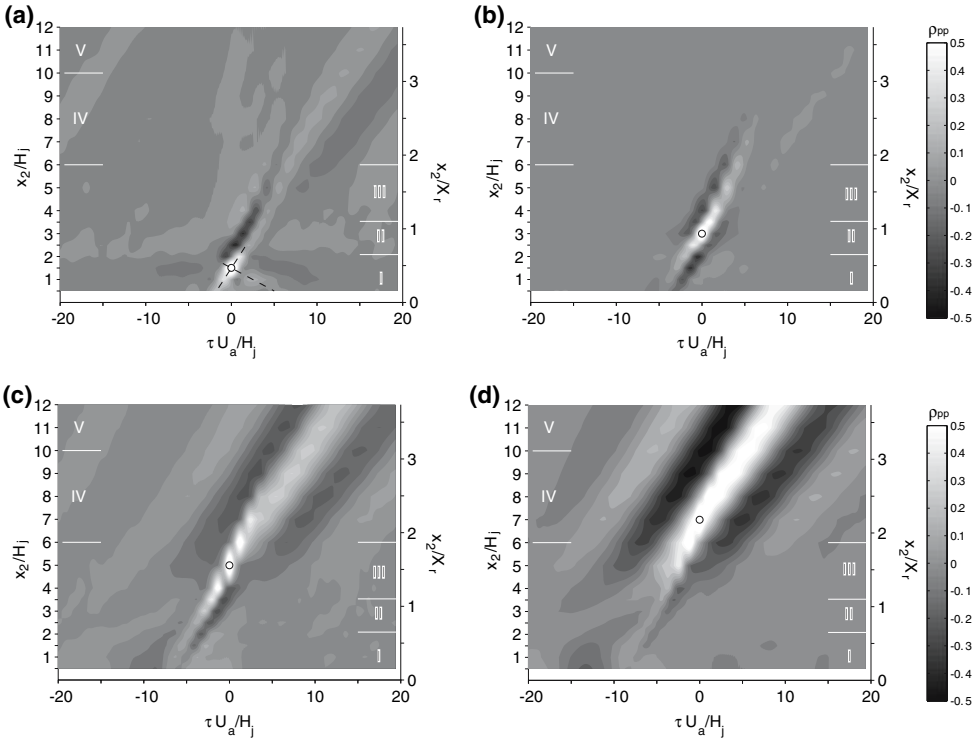

Fig. 12 Correlation coefficients, ρ_{pp}, of the fluctuating wall pressure for the reference microphone at x_1/H_j = ($x_1/X_r \approx$) **a** 1.5 (0.5) **b** 3 (1.0) **c** 5 (1.7) **d** 7 (2.1) for an offset jet with $H_s/H_j = 0.6$

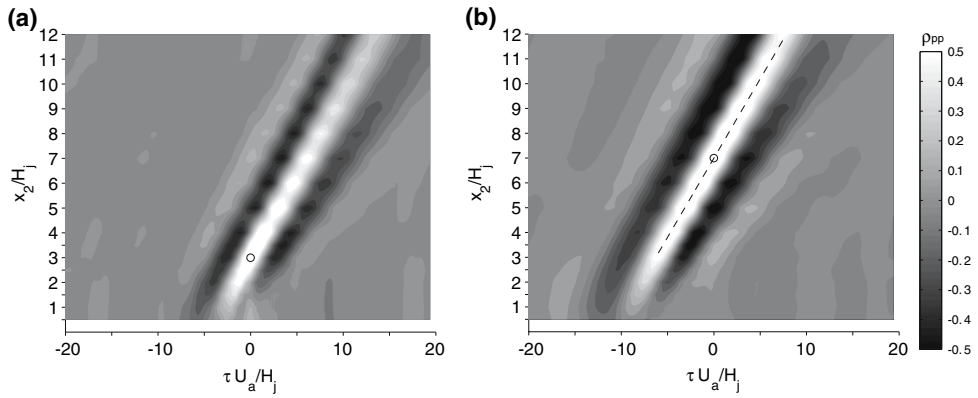

Fig. 13 Correlation coefficients, ρ_{pp}, of the fluctuating wall pressure for the reference microphone at x_1/H_j = **a** 3 and **b** 7 in the planar wall jet (with $H_s/H_j = 0$)

$x/H_j \approx 4$ ($x/X_r \approx 3.2$) in the jet with $H_s/H_j = 0.2$, and at $x/H_j \approx 8$ ($x/X_r \approx 1.8$) in the jet with $H_s/H_j = 1.0$. Thus, the transition in the structures downstream of the reattachment point does not correspond to the change in the development of the mean flow field, nor is it fixed in either x/X_r or x/H_j, likely because its position was determined by the prominence of the structures formed in the attaching shear layer and the wall jet flow.

The large scale structures can also be examined using the correlation coefficients between the fluctuating wall pressure at a position x_1 and the fluctuating velocities at different locations in the flow for time delays of τ; i.e.,

$$\rho_{pu} = \overline{p(x_1,t)u(x,y,t+\tau)}/p'(x_1)u'(x,y) \tag{3}$$

and

$$\rho_{pv} = \overline{p(x_1,t)v(x,y,t+\tau)}/p'(x_1)v'(x,y). \tag{4}$$

Contours of the correlation coefficients between the fluctuating velocities and the fluctuating wall pressure measured at $x_1/H_j = 2$ ($x_1/X_r = 0.43$) in the offset jet with $H_s/H_j = 1.0$ are shown in Fig. 15. These contours were generated from velocity measurements at 16×20 equally spaced locations. The areas with large positive and negative correlations are related to the large scale structures in the attaching shear layer flow. The results indicate that the structures are convected along the attaching shear layer and along the wall in the region $x/H_j \geq 6$ after the jet attaches to the wall.

The development of the structures downstream of the reattachment point can be examined using the correlation

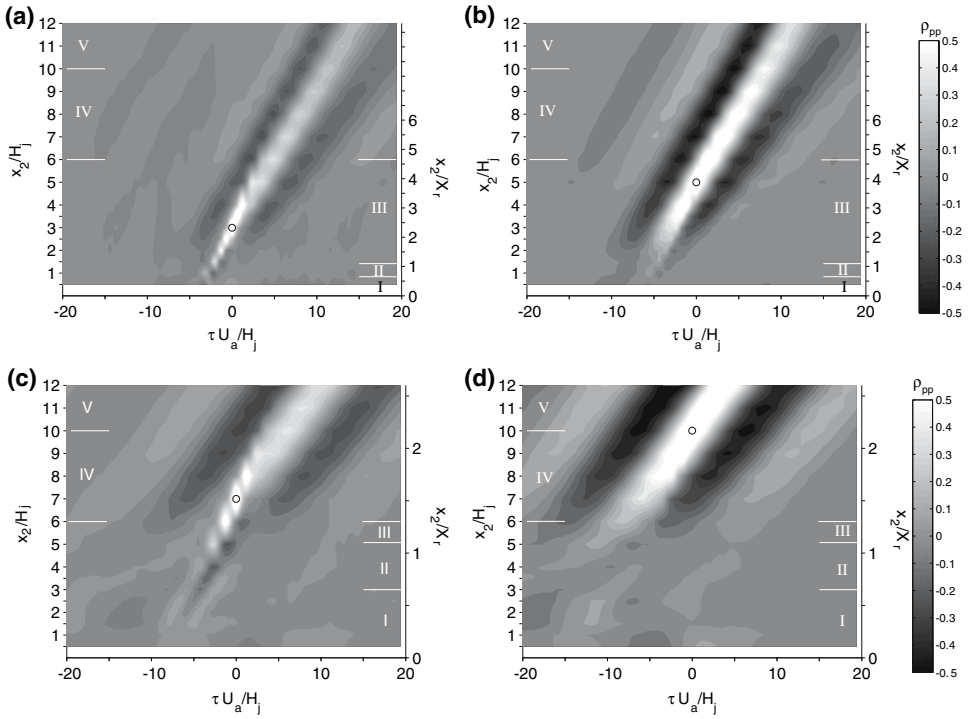

Fig. 14 Correlation coefficients, ρ_{pp}, of the fluctuating wall pressure with a reference microphone at x_1/H_j = ($x_1/X_r \approx$) **a** 3 (2.3) and **b** 5 (3.9) for the jet with H_s/H_j = 0.2 (*top*) and **c** 7 (1.5) and **d** 10 (2.2) for the jet with H_s/H_j = 1.0 (*bottom*)

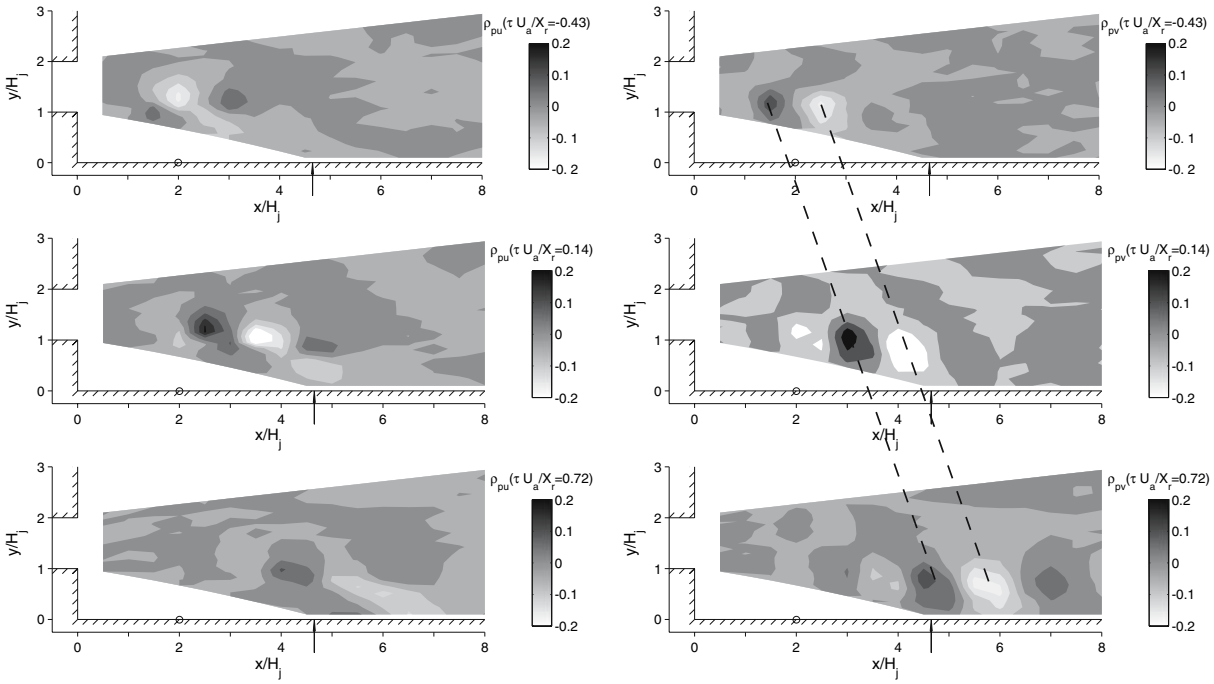

Fig. 15 Correlation coefficients ρ_{pu} (left) and ρ_{pv} (*right*) for the fluctuating wall pressure at x_1/H_j = 2 (x_1/X_r = 0.43) and the fluctuating velocities at different locations for time delays $\tau\ U_a/X_r \approx$ –0.43 to 0.72 in an offset jet with H_s/H_j = 1 and $Re \approx$ 44,000

coefficients between the fluctuating velocities and the fluctuating wall pressure measured at x_1/H_j = 8 shown in Fig. 16. These contours were generated from velocity measurements at 16×20 equally spaced locations at $x/H_j \leq 8$ and 8×20 equally spaced locations at $9 \leq x/H_j \leq 16$. In this case, the fluctuating pressure on the wall appears to be initially correlated with the fluctuating velocity associated with two different structures; larger structures that appear to span much of the outer jet, and smaller structures near the wall from the attaching shear layer. The

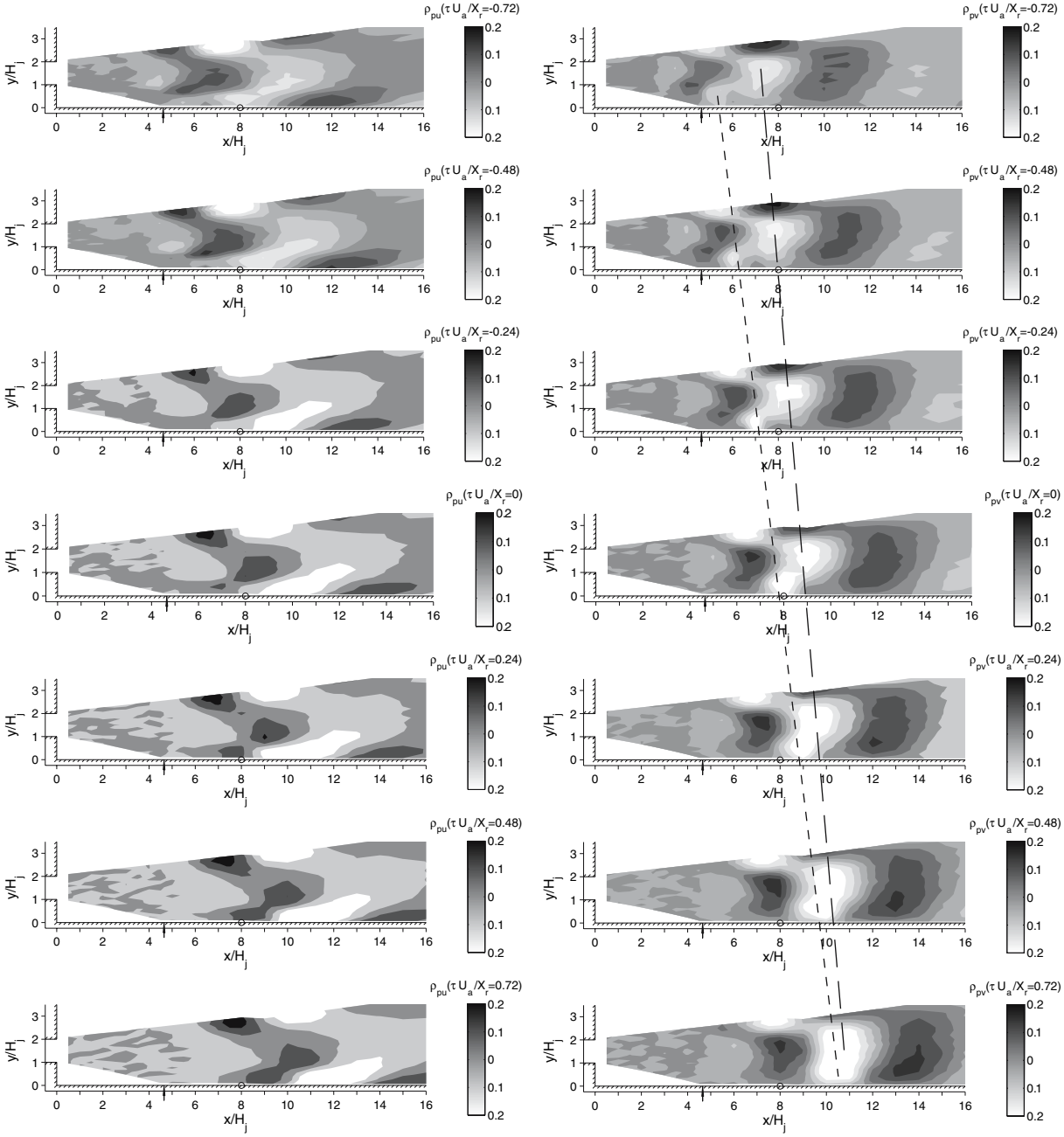

Fig. 16 Correlation coefficients ρ_{pu} (*left*) and ρ_{pv} (*right*) for the fluctuating wall pressure at $x_1/H_j = 8$ and the fluctuating velocities at different locations for time delays $\tau\ U_a/X_r \approx -0.72$ to 0.72 in an offset jet with $H_s/H_j = 1$ and $Re \approx 44{,}000$

results show that the smaller structures from the attaching shear layer are convected downstream faster than the larger outer structures causing the inner structure to approach the slower moving outer structure. The correlation measurements suggest that the two structures merge and travel downstream together in the region $x/H_j \geq 10$. The resulting correlations are similar to those observed in the planar wall jet shown in Fig. 17, indicating that the merged structures are similar to those that develop in the planar wall jet flow. Thus, the structures near the wall in the offset jet do transition from those associated with the attaching inner shear layer to lower frequency motions associated with the resulting wall jet flow.

The structures in the attaching shear layer and the wall jet region are both three-dimensional in nature. The three-dimensional development of the structures was examined in a separate investigation that considered the lateral correlation of the fluctuating velocity field and the fluctuating

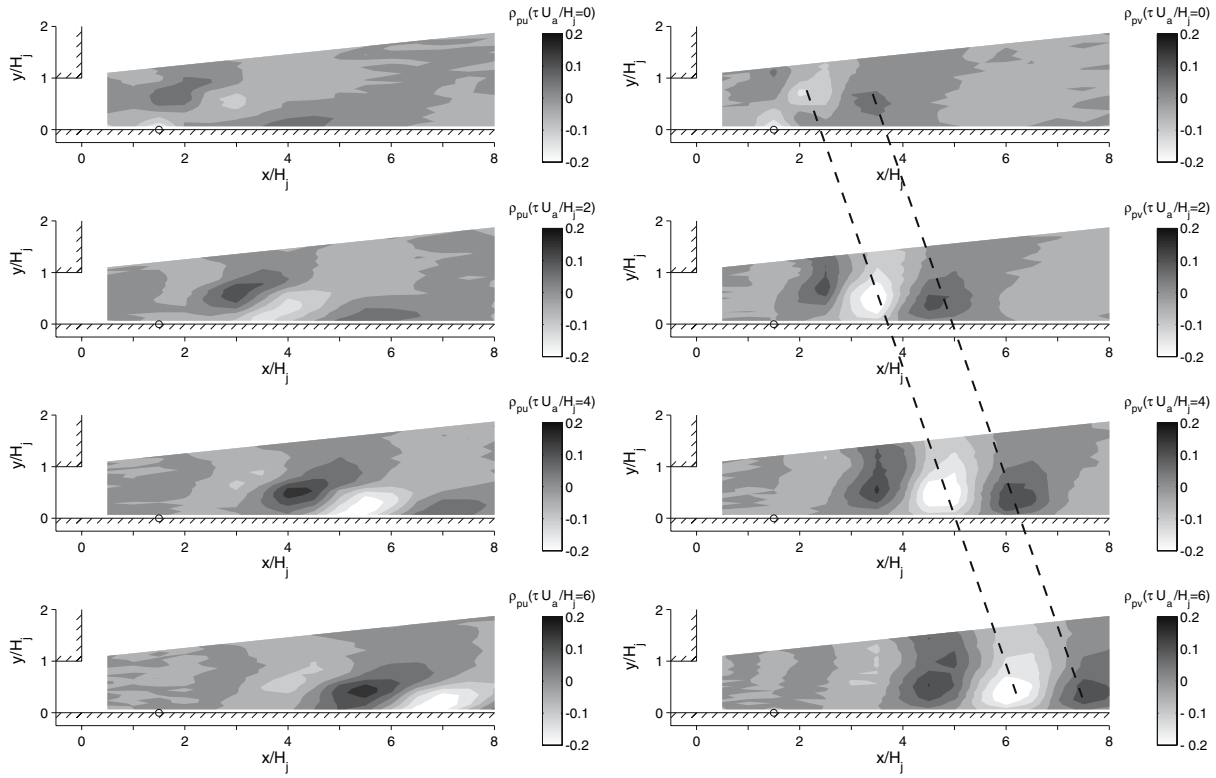

Fig. 17 Correlation coefficients ρ_{pu} (*left*) and ρ_{pv} (*right*) for the fluctuating wall pressure at $x_1/H_j = 1.5$ and the fluctuating velocities at different locations for time delays $\tau\ U_a/H_j \approx 0$–6 in the planar wall jet with $Re \approx 44{,}000$

wall pressure and fluctuating velocity field. The results showed that the integral length scale of the streamwise fluctuating velocity in the lateral direction was growing as the flow evolved downstream, and was approximately 0.3 H_j (or 1.5% of the facility width) in the core of the wall jet structure at $x/H_j = 16$ (from $y/H_j \approx 1.0$ to 2.2). Thus, it was thought that the three-dimensional development of the structures in the core region should not be affected by the width of the facility. The lateral correlations decayed more slowly outside this region indicating the spanwise roller structures played a more prominent role near the wall and in the outer region of the wall jet. The three-dimensional development of the structures will be considered in more detail in a later paper.

4 Concluding remarks

An experimental investigation was performed to characterize the development of planar jets issuing parallel to an adjacent wall with small offset distances. The results showed that the development of the mean flow field in the jets could be divided into five regions, three associated with the jet attaching to the wall, similar to other reattaching shear layer flows, and two associated with the development of the resulting planar wall jet flow. The results also showed that there was a change in the initial development of the attaching flow with the offset height, from one similar to a shear layer attaching to the wall to one more characteristic of a fully developed jet attaching to the wall. Evidence of this change was apparent in the reattachment length normalized by the offset height that was approximately 6 for jets with $H_s/H_j \lesssim 0.3$ similar to flows over a backward facing step, but decreased with offset distance at larger distances similar to fully developed jets attaching to a wall. The decay of the mean velocity and the recovery of the mean pressure in the jets with small offset distances after they attached to the wall were also more gradual than those in jets with larger offset distances.

The results showed that there is also a transition in the prominent structures near the wall as the flow develops downstream from those associated with the attaching inner shear layer to a lower frequency motion associated with the wall jet flow. Evidence of the change in the large-scale structures was observed in both the measurements of the fluctuating wall pressure and the correlation between the fluctuating pressure and the fluctuating velocities in the flow. The location of the transition in the structures did not correspond to the change in the development of the mean flow field, nor was it fixed in terms of x/X_r or x/H_j, likely

because its position was determined in part by the prominence of the structures formed in the attaching shear layer and the wall jet flow. The effect of the offset distance on the interaction between the structures in the inner and outer shear layers as well as the three-dimensional development of the structures will be considered in more detail in a later paper.

Acknowledgments This work was funded by the Natural Sciences and Engineering Research Council of Canada. The authors wish to acknowledge Prof. J. W. Naughton for his assistance in the measurements of the reattachment location, Dr. J. Hall for his suggestions, and Ms. L. C. Ofiara for her assistance in preparing the manuscript.

References

Beuther P (1980) Experimental investigation of the axisymmetric turbulent buoyant plume. PhD Thesis, The State University of New York at Buffalo, Buffalo, NY

Bourque C (1967) Reattachment of a two-dimensional jet to an adjacent flat plate. In: Brown FT (ed) Advances in fluidics. ASME Press, NY

Bourque C, Newman B (1960) Reattachment of a two-dimensional jet to an adjacent flat plate. Aeronaut Quart 11:201–232

Bruun H (1995) Hot-wire Anemometry. Oxford University Press, Oxford

Castro IP, Haque A (1987) The structure of a turbulent shear layer bounding a separation region. J Fluid Mech 179:439–468

Chandrsuda C, Bradshaw P (1981) Turbulence structure of a reattaching mixing layer. J Fluid Mech 110:171–194

Cherry N, Hillier R, Latour M (1984) Unsteady measurements in a separated and reattaching flow. J Fluid Mech 144:13–46

Citriniti J (1996) Experimental investigation into the large structures of the axisymmetric mixing layer using the proper orthogonal decomposition. PhD thesis, State University of New York at Buffalo, Amherts, NY

Driver D, Seegmiller H, Marvin J (1987) Time-dependent behavior of a reattaching shear layer. AIAA J 25:914–919

Eaton J, Johnson J (1981) A review of research on subsonic turbulent flow reattachment. AIAA J 19:1093–1100

Farabee T, Casarella M (1986) Measurements of fluctuating wall pressure for separated/reattached boundary layer flows. J Vib Acous Stress Reliab Des 108:301–307

Gao N, Ewing D (2005) Investigation of the large-scale flow structures in the cooling jets used in the blown film manufacturing process. J Fluids Eng 127:978–985

Gao N, Li S, Ewing D (2005) Experimental investigation of cooling jets used in the blown film manufacturing process. Int Polymer Process 20:68–77

Heenan A, Morrison J (1998) Passive control of pressure fluctuations generated by separated flow. AIAA J 36:1014–1022

Hoch J, Jiji M (1981) Two-dimensional turbulent offset jet boundary interaction. J Fluids Eng 103:154–161

Hudy L, Naguib A, Humphreys W (2003) Wall-pressure-array measurements beneath a separating/reattaching flow region. Phys Fluids 15:706–717

Kim D, Yoon S, Lee D, Kim K (1996) Flow and heat transfer measurements of a wall attaching offset jet. Int J Heat Mass Transf 39:2907–2913

Kiya M, Sasaki K (1983) Structure of a turbulent separation bubble. J Fluid Mech 137:83–113

Kiya M, Sasaki K (1985) Structure of large-scale vortices and unsteady reverse flow in the reattaching zone of a turbulent separation bubble. J Fluid Mech 154:463–491

Lee I, Sung J (2002) Multiple-arrayed pressure measurement for investigation of the unsteady flow structure of a reattaching shear layer. J Fluid Mech 463:377–402

Lund T (1986) Augmented thrust and mass flow associated with two-dimensional jet reattachment. AIAA J 24:1964–1970

Nasr A, Lai J (1997) Comparison of flow characteristics in the near field of two parallel plane jets and an offset plane jet. Phys Fluids 9:2919–2931

Nasr A, Lai J (1998) A turbulent plane offset jet with small offset ratio. Exp Fluids 24:47–57

Naughton J, Sheplak M (2002) Modern developments in shear stress measurement. Prog Aerosp Sci 38:515–570

Nozaki T, Hatta K, Nakashima M, Matsumura H (1979) Reattachment flow issuing from a finite width nozzle. Bull JSME 22:340–347

Nozaki T, Hatta K, Sato N, Matsumura H (1981) Reattachment flow issuing from a finite width nozzle, report 2 effect of initial turbulence intensity. Bull JSME 24:363–369

Pelfrey J, Liburdy J (1986) Mean flow characteristics of a turbulent offset jet. J Fluids Eng 108:82–88

Perry A (1982) Hot-wire anemometry. Clarendon Press, Oxford

Ruderich R, Ferngolz HH (1986) An experimental investigation of a turbulent shear flow with separation, reverse flow, and reattachment. J Fluid Mech 163:283–322

Sawyer R (1960) The flow due to a two-dimensional jet issuing parallel to a flow plate. J Fluid Mech 9:543–560

Sawyer R (1963) Two-dimensional reattachment jet flows including the effect of curvature on entrainment. J Fluid Mech 17:481–498

Song H, Yoon S, Lee D (2000) Flow and heat transfer characteristics of a two-dimensional oblique wall attaching offset jet. Int J Heat Mass Transf 43:2395–2404

Spazzini P, Iuso G, Onorato M, Zurlo N, Di-Cicca G (2001) Unsteady behavior of back-facing step flow. Exp Fluids 30:551–561

Tutu NK, Chevary R (1975) Cross-wire anemometry in high intensity turbulence. J Fluid Mech 71:785–800

Vogel JC, Eaton JK (1985) Combined heat transfer and fluid dynamic measurements downstream of a backward-facing step. J Heat Transf 107:922–929